Inorganica Chimica Acta 385 (2012) 73–80

Contents lists available at SciVerse ScienceDirect

Inorganica Chimica Acta

journal homepage: www.elsevier.com/locate/ica

Synthesis, structure, magnetic properties and DFT calculations of novel bis-(5-tetrazolyl)amine copper(II) complexes

Antonio Rodríguez-Diéguez *, Marta E. López-Viseras, Jesús E. Perea-Buceta, Antonio J. Mota, Enrique Colacio

Departamento de Quimica Inorganica, Universidad de Granada, 18071 Granada, Spain

ARTICLE INFO

Article history:
Received 12 October 2011
Received in revised form 20 December 2011
Accepted 21 December 2011
Available online 5 January 2012

Keywords:
BTA
Copper complexes
Magnetic properties
DFT calculations

ABSTRACT

Four new multidimensional copper(II) complexes [Cu(BTA)(2,2′-bipy)H_2O] (**1**), [Cu(BTA)(1,10′-phen)] (**2**), [$Cu_2(BTA)_2(H_2O)_4$] (**3**) and $[Cu(BTA)(en)]_n$ (**4**) have been synthesized by conventional and hydrothermal reactions of the bis(5-tetrazolyl)amine (H_2BTA) with copper(II) salts in the presence of different ancillary ligands. X-ray diffraction studies on these compounds show **1** and **2** are mononuclear entities, in which the BTA ligand acts in a chelate coordination mode and the copper atoms exhibit a coordination environment intermediate between trigonal-bipyramidal and square-pyramidal for **1** and between square-planar and tetrahedral for **2**. Complex **3** consists of centrosymmetric dinuclear molecules with the ligand acting in a μ_2-1,1′:2 chelate/bridging tridentate coordination mode and **4** is a linear zigzag neutral chain bearing a BTA bridging ligand in a μ_2-1,1′:3 chelate/bridging tridentate coordination mode. Complexes **3** and **4** exhibit antiferromagnetic and very weak ferromagnetic interactions, respectively. DFT calculations have been performed in order to explain their respective magnetic behaviors.

1. Introduction

Tetrazole-derived ligands have attracted much attention in recent years not only due to their rich coordination chemistry that has provided a great variety of fascinating and intriguing structures but also due to their interesting optical, magnetic and hydrogen storage properties and potential energetic applications [1]. In 2001, Sharpless and Demko reported an environmentally friendly process for the preparation of 5-substituted 1H-tetrazoles via metal-assisted 1,3-dipolar cycloaddition of nitriles and azides [2]. After that numerous tetrazole ligands have been prepared and structurally characterized [3]. Recently, we and others showed the ability of the versatile 5-pyrimidyl-tetrazolate (pmtz) and tetrazole-5-carboxylic acid (H_2TzC) ligands to produce M^{II} (Co^{II}, Fe^{II}, Cd^{II} and Cu^{II}) multidimensional coordination polymers with interesting magnetic [4], zeolitic [5] and photoluminescence properties [6]. These ligands possess six and four nitrogen donor atoms, respectively, and consequently exhibit a wide diversity of potential coordination modes. In view of the above considerations, we have decided to prepare a polytopic ligand, bis(5-tetrazolyl)amine (H_2BTA) (Scheme I) to perform a systematic study of its coordination chemistry with copper salts. The aim of this work is to know how the great plasticity of the copper coordination sphere influences the formation of different structures. Notice that only a few copper(II) complexes bearing this ligand have been reported so far [7].

In principle, the BTA^{2-} ligand is an ideal candidate for obtaining polymeric frameworks with intriguing structures and interesting physical properties because it has nitrogen donor atoms which could provide a wide variety of potential coordination modes [8]. By changing the metal ions and their charges we could expect to obtain coordination complexes with great structural diversity.

We report here on the preparation, structural characterization, magnetic properties and some DFT calculations of the following BTA-containing copper(II) complexes: [Cu(BTA)(2,2′-bipy)H_2O] (**1**), [Cu(BTA)(1,10′-phen)] (**2**), [$Cu_2(BTA)_2(H_2O)_4$] (**3**) and $[Cu(BTA)(en)]_n$ (**4**). **1** and **2** are mononuclear complexes, **3** is a centrosymmetric dinuclear complex and **4** is a linear zigzag neutral chain.

2. Experimental

2.1. General

All analytical reagents were purchased from commercial sources and used without further purification. Perchlorate salts are potentially explosive and only should be handled in small quantities.

Abbreviations: H_2BTA, bis(5-tetrazolyl)amine; 2,2′-bipy, 2,2′-bipyridine; 1,10′-phen, 1,10′-phenantroline; en, ethylenediamine.

* Corresponding author. Tel.: +34 958240442.

E-mail address: antonio5@ugr.es (A. Rodríguez-Diéguez).

0020-1693/$ - see front matter © 2012 Elsevier B.V. All rights reserved.
doi:10.1016/j.ica.2011.12.040

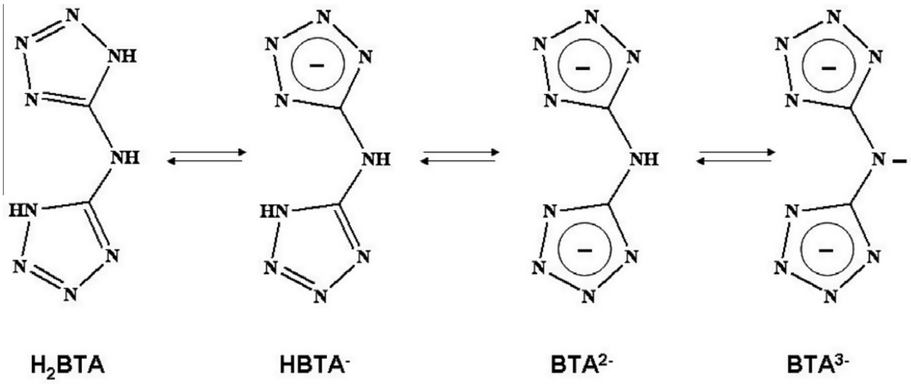

Scheme I. H_2BTA with three reversible types of protonated, deprotonated, triprotonated mode.

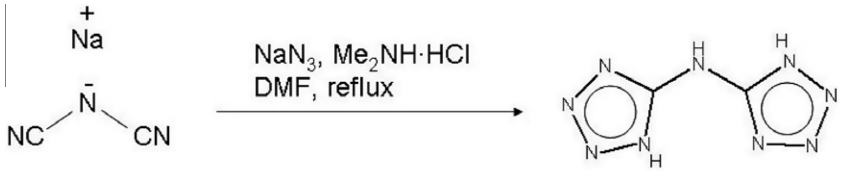

Scheme II. Synthesis of bis(5-tetrazolyl)amine (H_2BTA).

2.2. Synthesis of bis(5-tetrazolyl)amine (H_2BTA)

Bis(5-tetrazolyl)amine was prepared according to the procedure reported by Zubarev et al. [9] by refluxing dicyanamide and sodium azide in dry *N*,*N*-dimethylformamide (Scheme II).

2.3. Preparation of the complexes

2.3.1. [Cu(BTA)(2,2′-bipy)H2O] (1)

An aqueous solution of $Cu(ClO_4)_2{\cdot}6H_2O$ (0.183 g, 0.49 mmol, in 20 mL H_2O) was added under continuous stirring to an aqueous solution of 2,2′-bipyridine (0.077 g, 0.49 mmol, in 20 mL H_2O). After stirring the resulting suspension for 15 min, H_2BTA (0.100 g, 0.49 mmol, in 20 mL H_2O) was added. The resulting green solution was stirred for 20 min and then it was left standing at room temperature for 10 days. Green crystals of **1** formed, which were filtered off and air dried. The yield was 15% based on copper. *Anal.* Calc. for $C_{12}H_{11}N_{11}OCu$: C, 37.07; H, 2.85; N, 39.62. Found: C, 36.95; H, 2.80; N, 39.65%. IR (KBr, cm^{-1}): ν 3321 (s), 3138 (m), 2925 (m), 1621 (vs), 1535 (s), 1489 (s).

2.3.2. [Cu(BTA)(1,10′-phen)] (2)

Hydrothermal treatment of a mixture containing $Cu(ClO_4)_2{\cdot}6H_2O$ (0.183 g, 0.49 mmol), 1,10-phenantroline (0.098 g, 0.49 mmol), H_2BTA (0.100 g, 0.49 mmol) and water (10 mL) at 150 °C for four hours gave rise to a green-pale solution, which kept at room temperature for 5 days, afforded green-dark crystals of **2**. The yield was 21% based on copper. *Anal.* Calc. for $C_{28}H_{18}N_{22}Cu_2$: C, 42.59; H, 2.30; N, 39.02. Found: C, 42.13; H, 2.21; N, 38.97. IR (KBr, cm^{-1}): ν 3141 (m), 1617 (vs), 1531 (s), 1481 (s).

2.3.3. [Cu2(BTA)2(H2O)4] (3)

To a solution of copper acetate (0.099 g, 0.49 mmol in 20 mL of water) was added a solution of H_2BTA (0.100 g, 0.49 mmol in 20 mL H_2O). The resulting green solution was additionally stirred for 20 min. and then was left standing at room temperature for 5 days. Green crystals of **3** formed, which were filtered off and air dried. Yield: 60%. *Anal.* Calc. for $C_4H_{10}N_{18}O_4Cu_2$: C, 9.58; H, 2.01; N, 50.29. Found: C, 9.53; H, 1.98; N, 50.27%. IR (KBr, cm^{-1}): ν 3335 (s), 3241 (m), 3139 (m), 2923 (m), 1629 (vs), 1531 (s), 1485 (s).

2.3.4. [Cu(BTA)(en)]n (4)

A mixture of $Cu(ClO_4)_2{\cdot}6H_2O$ (0.183 g, 0.49 mmol), H_2BTA (0.100 g, 0.49 mmol), ethylenediamine (1 ml) and water (10 mL) was added to a Teflon-lined stainless steal Parr acid digestion vessel and heated at 150 °C for 4 h under autogenous pressure. After slow cooling to room temperature, blue crystals of **4** were recovered. Yield: 40%. *Anal.* Calc. for $C_4H_9N_{11}Cu$: C, 17.49; H, 3.30; N, 56.08. Experimental: C, 17.43; H, 3.19; N, 55.78%. IR (KBr, cm^{-1}): ν 3328 (s), 3247 (m), 3131 (m), 2921 (m), 2817 (m), 1625 (vs), 1539 (s), 1491 (s), 1323 (m).

2.4. Physical measurements

Elemental analyses were carried out at the "Centro de Instrumentación Científica" (University of Granada) on a Fisons-Carlo Erba analyser model EA 1108. The IR spectra on powdered samples were recorded with a ThermoNicolet IR200FTIR by using KBr pellets. Magnetization and variable temperature (1.9–300 K) magnetic susceptibility measurements on polycrystalline samples were carried out with a Quantum Design SQUID MPMS XL-5 device operating at different magnetic fields. The experimental susceptibilities were corrected for the diamagnetism of the constituent atoms by using Pascal's tables.

2.5. Single-crystal structure determination

Suitable crystals of **1**–**4** were mounted on glass fiber and used for data collection. Data were collected with a Bruker AXS APEX CCD area detector equipped with graphite monochromated Mo K radiation (λ=0.71073 Å) by applying the ω-scan method. The data were processed with APEX2 [10] and corrected for absorption using SADABS [11]. The structures were solved by direct methods using SIR97 [12], revealing positions of all non-hydrogen atoms. These atoms were refined on *F*2 by a full matrix least-squares procedure

Table 1
Crystallographic data structural refinement details for **1**–**4**.

Compound	1	2	3	4
Chemical formula	$C_{12}H_{11}N_{11}OCu$	$C_{14}H_9N_{11}Cu$	$C_4H_{10}N_{18}O_4Cu$	$C_4H_9N_{11}Cu$
M/gmol^{-1}	388.86	394.86	501.38	274.76
T (K)	293	293	293	293
λ (Å)	0.71073	0.71073	0.71073	0.71073
Crystal system	triclinic	triclinic	triclinic	monoclinic
Space group	$P\bar{1}$	$P\bar{1}$	$P\bar{1}$	P21/C
Unit cell dimensions				
a (Å)	7.879(2)	7.105(5)	5.475(5)	8.422(1)
b (Å)	11.621(3)	9.091(5)	7.635(5)	11.607(2)
c (Å)	16.539(4)	12.017(5)	9.229(5)	9.873(2)
α (°)	85.749(3)	76.156(5)	78.272(5)	90
β (°)	82.585(3)	87.455(5)	81.872(5)	95.724(2)
γ (°)	80.756(3)	70.722(5)	83.331(5)	90
V (A^3)	1480.0(6)	710.9(7)	372.4(5)	960.3(3)
Z	4	2	1	4
ρ (g cm^{-3})	1.745	1.845	2.236	1.901
μ (mm^{-1})	1.506	1 565	2.926	2.269
Unique reflections	5811	6958	3709	9039
R_{int}	0.000	0.023	0.058	0.037
GOF on F^a	1.051	1.059	1.023	1.066
R_1 [$I > 2\sigma(I)$]	0.033	0.028	0.046	0.029
wR_2 [$I > 2\sigma(I)$]	0.071	0.075	0.093	0.071

[a] $R(F) = \Sigma||F_o| - |F_c||/\Sigma|F_o|$, $wR(F^2) - [\Sigma w(F_o^2 - F_c^2)^2/\Sigma wF^4]^{1/2}$.

using anisotropic displacement parameters [13]. All hydrogen atoms were located in difference Fourier maps and included as fixed contributions riding on attached atoms with isotropic thermal displacement parameters 1.2 times those of the respective atom. Final $R(F)$, $wR(F^2)$ and goodness of fit agreement factors, details on the data collection and analysis can be found in Table 1.

2.6. Computational details

All theoretical calculations were carried out at the DFT level of theory using the hybrid B3LYP exchange-correlation functional [14], as implemented in the GAUSSIAN 03 program [15]. A quadratic convergence method was employed in the SCF process [16]. All-electron, triple-ζ quality basis set proposed by Ahlrichs and co-workers has been used for all atoms [17]. The calculations were performed on the complexes **3** and **4** built from the experimental geometries. The electronic configurations used as starting points were created using Jaguar 7.6 software [18]. The approach that we used herein to determine the exchange coupling constants has been described in detail elsewhere [19].

3. Results and discussion

3.1. Descriptions of crystal structures

The structure of **1** consists of two neutral monomeric molecules of [Cu(BTA)(2,2′-bipy)H_2O] (A and B) which are shown in Fig. 1. The copper ion exhibits a CuN_4O coordination environment which is formed by the coordination of two nitrogen atoms from the bidentate bipy ligand and two nitrogen atoms (N1 and N6) belonging to the dideprotonated BTA^{2-} tetrazolate ligand. The fifth position is occupied by a water molecule. Bond distances and angles are similar in both mononuclear units. Cu–N(2,2′-bipy) distances range from 1.992(2) to 2.055(2) Å, whereas Cu–N(BTA) distances are in the range 1.963(2)–1.994(2) Å. The Cu–O(w) axial distances are 2.180(2) and 2.236(2) Å for molecules A and B, respectively. The

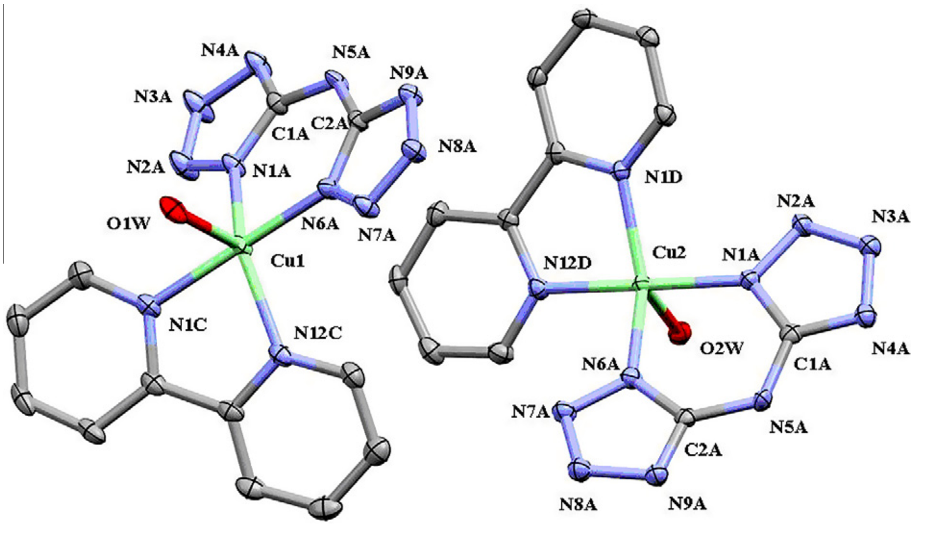

Fig. 1. The structure of the [Cu(BTA)(2,2′-bipy)H_2O] (**1**). Thermal ellipsoids are drawn at the 35% probability level. Hydrogen atoms have been omitted for clarity.

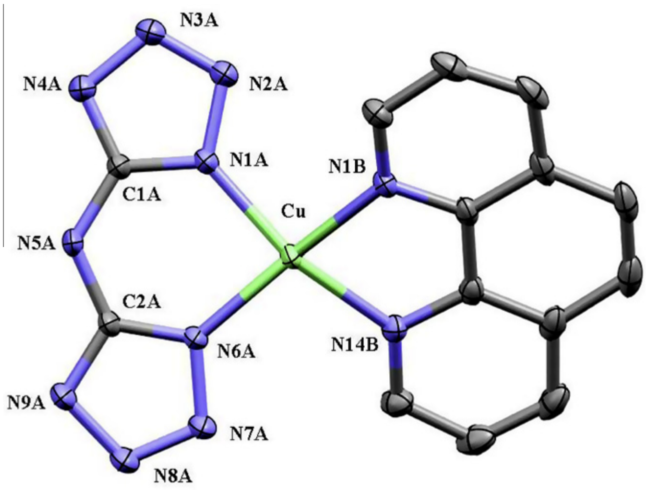

Fig. 2. View of the molecular structure of complex **2**. Thermal ellipsoids are drawn at the 50% probability level. Hydrogen atoms have been omitted for clarity.

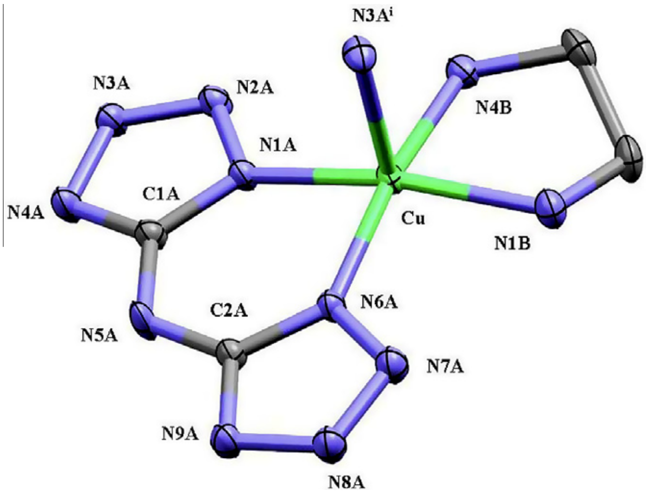

Fig. 4. Coordination environment of the Cu^{II} ion in **4**, showing the atom numbering scheme. Displacement ellipsoids are drawn at the 50% probability level, and H atoms are shown as spheres of arbitrary radii. (Symmetry code: (i) $-0.5 - x$, $0.5 + y$, $0.5 - z$).

trans angles in the equatorial plane N1A–Cu1–N12C, N6A–Cu1–N1C, N1B–Cu2–N12D, N6B–Cu2–N1D are of 141.99(9), 175.03(9), 173.29(9) and 143.94(9), respectively.

The coordination geometry around copper atoms is intermediate between trigonal-bipyramidal (TBPY5) and square-pyramidal (SPY5) ($\tau = 0.55$ and 0.49 for Cu1 and Cu2, respectively, $\tau = 1$ for TPY5 and $\tau = 0$ for SPY5) [20].

The coordinated water molecule in both molecules A and B is involved in hydrogen bonds interactions with the nitrogen atoms N4 and N8 from BTA ligands belonging to neighbor units of the same type (A and B). These interactions give rise to the formation of two 1D hydrogen bonded chains. Moreover, in these 1D systems there are intrachain H-bonded interactions between N5 and N9. The distances between the donor atoms involved in hydrogen bond interactions are given in Table SI2. The crystal packing of the chains is further stabilized by face-to-face $\pi \cdots \pi$ interactions involving tetrazolate rings. Moreover, polymeric chains A and B are stacked in such a way that centroid–centroid distances between bipyridine rings are near to 3.340 Å.

The crystal structure of molecule **2** consists of discrete neutral [Cu(BTA)(1,10′-phen)] molecules. A perspective view of **2** is shown in Fig. 2 and selected bond distances and angles are listed in Table SI1. The CuN_4 environment around each copper(II) atom is close to being half way between square-planar (D_{4h}) and tetrahedral (T_d) with a δ value of 0.79 ($\delta = \Delta/70.5$, Δ being the difference between the mean value of the *trans* N–Cu–N angles and the ideal tetrahedral angle of 109.5°; $\delta = 0$ for the ideal tetrahedral geometry and $\delta = 1$ for the ideal square planar geometry).

The copper(II) ion is coordinated by two nitrogen atoms belonging to the BTA^{2-} ligand (Cu–N1A = 1.951(2) Å and Cu–N6A = 1.950(2) Å) and two nitrogen atoms (Cu–N1B = 1.991(2) Å and Cu–N14B = 2.016(2) Å) from the phenanthroline ligand. The *cis* bond angles are in the range 82.00(8)–100.84(8)°, while the *trans* bond angles have values of 154.77(9) and 165.39(8)°. Centrosymmetric related molecules of **2** are hold together by a pair of complementary hydrogen bonds involving the N5 amine nitrogen atom of a molecule and the N9 atom of the neighboring unit (donor–acceptor distance of 2.867 Å) to form dinuclear species. The crystal packing of the dinuclear copper complexes is stabilized by face-to-face interactions between two phenantroline rings with centroid–centroid distances near to 3.320 Å, ultimately leading to 1D chains along the [0 1 1] direction.

The structure of the compound $[Cu_2(BTA)_2(H_2O)_4]$ (**3**) consists of centrosymmetric dinuclear molecules $[Cu_2(BTA)_2(H_2O)_4]$ with C_i symmetry (Fig. 3) which are involved in an extensive network of hydrogen bonds, ultimately affording a 3D structure. Within the dinuclear unit, copper(II) atoms are bridged by two BTA^{2-} anions and each metal ion exhibits a square-pyramidal SPY5 CuN_3O_2 coordination environment, which is formed by the coordination in the same plane of the N1 and N6 tetrazolato nitrogen atoms in the *cis* position of the same BTA ligand, giving rise to a stable six-membered chelate ring, the N2 tetrazolate nitrogen atom belonging to a symmetry related BTA^{2-} anion, which is located in *trans* position to the N6 nitrogen atom, one water molecule (O2 W) in *trans*

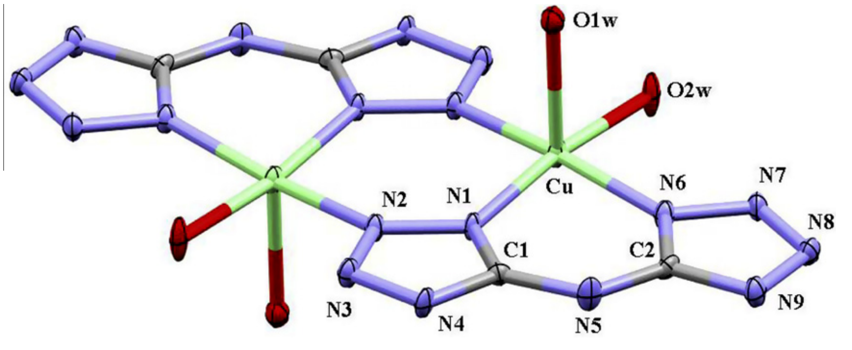

Fig. 3. View of the structure of **3**. Thermal ellipsoids are drawn at the 50% probability level H-atoms are omitted for the sake of clarity.

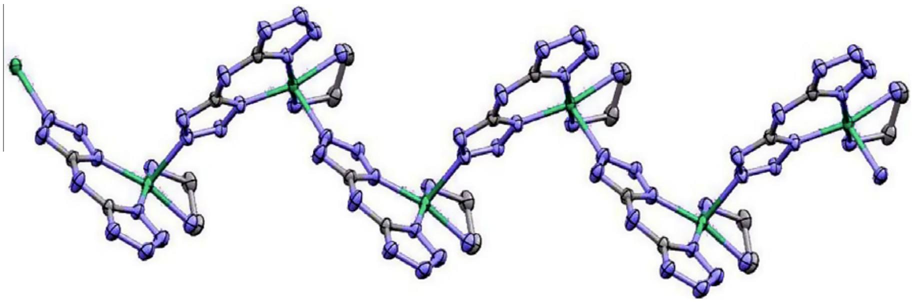

Fig. 5. View of the chain along the *c* axis on the structure of **4**. Thermal ellipsoids are drawn at the 50% probability level H-atoms are omitted for the sake of clarity. Copper(II), nitrogen and carbon atoms are green, blue and gray, respectively.

positions to the N1 nitrogen atom and a molecule of water (O1 W) in apical position. Therefore, the ligands exhibit a μ_2-1,1′:2 chelating/bridging tridentate coordination mode, which generates a centrosymmetric planar Cu(N–N)$_2$Cu hexagon with Cu$\cdots$Cu distances of 4.012 Å, respectively. This structure is similar to the binuclear motif of the chain [Zn(BTA)(NH$_3$)$_2$]·0.5H$_2$O [8] and to that formed for the dinuclear complex [Cu$_2$(TzC)$_2$(H$_2$O)$_6$] (TzC = 5-tetrazolate-carboxylate dianion) [21].

Bond distances around Cu(II) atoms are shown in the Table SI1 with values of 1.984(4), 1.981(4), 1.953(4), 1.981(5) and 2.330(5) Å for Cu–N1, Cu–N2, Cu–N6, Cu–O2 W and Cu–O1 W bond distances, respectively. *Trans* N2–Cu–N6 and N1–Cu–O2 W bond angles are significantly deviated from linearity (168.45(17)° and 172.8(2)°) and consequently the *trans*-coordinated water molecule (O2 W) is 0.186 Å out from the equatorial plane. It should be noted that this complex displays asymmetric double tetrazolato bridges, as the Cu–N1–N2 and Cu–N2–N1 angles are different (130.1(3)° and 132.6(3)°). In this compound, with the exception of the coordinated nitrogen atoms, N3 and N7, all donor atoms of the BTA^{2-} ligand are involved in hydrogen bonds with the coordinated water molecules and the N5–H group of neighboring dinuclear molecules, giving rise to a intrincate 3D network (Fig. SI3). It should be noted that the shortest hydrogen bond is established between the water molecules O1 W and O2 W with a value of 2.758 Å.

In the chain compound [Cu(BTA)(en)]$_n$ (**4**) each Cu(II) ion is five coordinate (Fig. 4) and exhibits an almost perfect CuN$_5$ square-pyramidal coordination geometry (τ = 0.036). The basal plane is formed by the nitrogen atoms N1A and N6A belonging a BTA ligand, and the nitrogen atoms from the coordinated ethylenediamine molecule. A nitrogen atom from a neighbor molecule (N3A^i) occupies the apical position (symmetry code: (i) $-0.5-x$, $0.5+y$, $0.5-z$) at longer distance of 2.256(2) Å, and connects [Cu(BTA)(en)] units to form a zig-zag chain (Fig. 5).

The Cu–N bond lengths involving the nitrogen atoms of the BTA ligand with values of 1.966(2) and 1.975(2) Å (Table SI1), which are slightly shorter than the Cu–N bond lengths involving the coordinated nitrogen atoms pertaining to the ethylenediamine ligand (2.010(2) and 2.024(2) Å) and are similar to those observed in comparable copper complexes containing tetrazolate or ethylenediamine ligands [22]. The copper atom is not in the basal plane, but it is located 0.230 Å out of the mean basal plane toward N3*i*.

Chains of **4** are oriented in such way that there exist face-to-face $\pi\cdots\pi$ interactions between centrosymmetric related tetrazolate rings with centroid–centroid distances of about 3.480 Å and hydrogen bond interactions involving the N5 and N4 nitrogen atoms of centrosymmetric related BTA^{2-} ligands with donor–acceptor distances of 2.947 Å. These interactions generate a complicated 3D network.

3.2. Magnetic properties

The magnetic properties of the complex [Cu$_2$(BTA)$_2$(H$_2$O)$_4$] (**3**) in the form $\chi_M T$ versus T (χ_M is the molar magnetic susceptibility per dinuclear copper(II) unit) are shown in Fig. 6.

The $\chi_M T$ product at room temperature of 0.91 cm^3 K mol^{-1} is close to the expected value for two uncoupled Cu^{II} atoms with g = 2.18 (0.89 cm^3 K mol^{-1}). On lowering the temperature, the $\chi_M T$ product steadily decreases until 50 K and then decreases deeply tends toward zero at 2 K. This behavior indicates the existence of a weak antiferromagnetic interaction through the tetrazolato bridging ligand leading to a S = 0 ground state. The susceptibility data were analyzed using the Bleaney–Bowers expression for two magnetically interacting spin doublets derived from the isotropic Hamiltonian:

$$\hat{H} = -J\hat{S}_1\hat{S}_2 + g\beta H(\hat{S}_1\hat{S}_2)$$

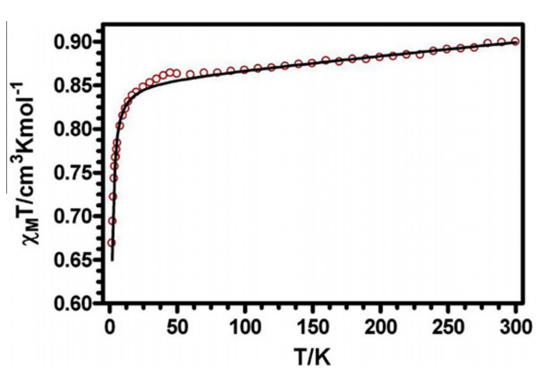

Fig. 6. Temperature dependence of $\chi_M T$ for **3** under an applied magnetic field of 0.5 *T*. Solid lines represent the best fit of the date with the model described in the text.

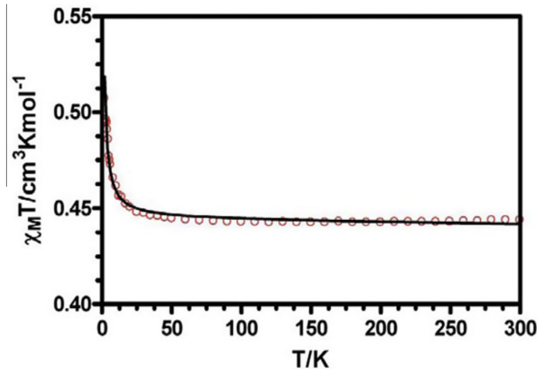

Fig. 7. Temperature dependence of $\chi_M T$ for **4** under an applied magnetic field of 0.5 *T*. Solid lines represent the best fit of the date with the model described in the text.

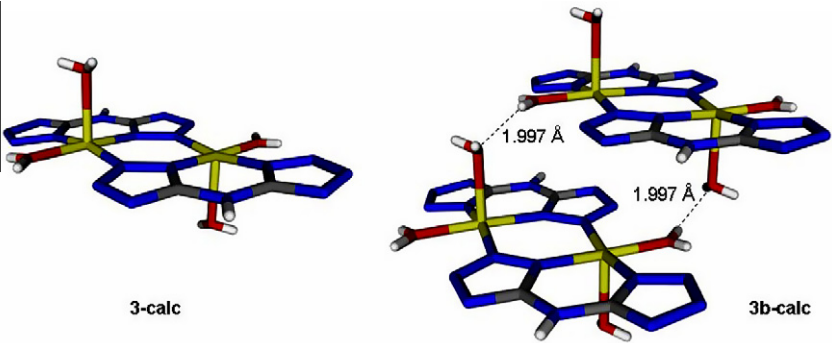

Fig. 8. The units calculated for complex **3**.

Least-squares best-fit results were: $J = -1.13(2)\ \mathrm{cm}^{-1}$, $g = 2.135(2)$. Therefore, the antiferromagnetic interaction mediated by the bridging tetrazolate ligand is very weak.

The magnetic susceptibility of the $[\mathrm{Cu(BTA)(en)}]_n$ (**4**) complex has been measured over the temperature range of 300–2 K. The temperature dependence of $\chi_M T$ (χ_M being the susceptibility for copper(II) atom) is shown in Fig. 7.

The $\chi_M T$ product at room temperature of $0.445\ \mathrm{cm^3\ K\ mol^{-1}}$ is slightly larger than the spin-only value of $0.37\ \mathrm{cm^3\ K\ mol^{-1}}$ expected for a single copper(II) ion ($S = 1/2$), assuming $g = 2.00$. Upon cooling down $\chi_M T$ increases continuously from room temperature until reaching a value of $0.51\ \mathrm{cm^3\ K\ mol^{-1}}$ at 2 K. This behavior support the existence of a weak ferromagnetic interaction between the paramagnetic centres. To estimate the magnitude of the ferromagnetic coupling, the magnetic data were fitted using the expression proposed by Baker et al. for a ferromagnetic chain with $S = 1/2$ [23]

$$H = -J\sum_{i=1}^{n-1} S_{Ai}S_{Ai+1}$$

From the best fit to the following parameters $J = +0.233(9)\ \mathrm{cm}^{-1}$, $g = 2.180(2)$.

The magnetic coupling in this compound takes place through the tetrazolate bridging ligand involving basal(short)-axial (long) positions on neighboring copper(II) atoms. This exchange pathway always leads to very small coupling (either antiferro- or ferromagnetic) regardless of the structural parameters of the bridge. This is due to the long axial Cu–N distance and to the fact that the spin density of the unpaired electron at axial position is, if any, negligible (the magnetic orbitals on the Cu(II) atoms of the $dx^2 - y^2$ type are mainly located in the equatorial plane and directed to the nitrogen atom of the ethylenediamine and tetrazolate ligands). In the case of compound **4**, that exhibits an almost perfect square-pyramidal geometry, the observed ferromagnetic behavior is therefore not unexpected.

3.3. DFT calculations

DFT calculations have been performed on complexes **3** and **4** in order to evaluate the corresponding theoretical J values. For compound **3**, just the dimer **3**-calc. (Fig. 8) has been initially considered, for which it has been determined a J value of $+4.8\ \mathrm{cm}^{-1}$, which differs in sign from the experimental value of $-1.13\ \mathrm{cm}^{-1}$.

When intermolecular interactions through hydrogen bonds (involving coordinated water molecules) are, however, taken into account by calculating the dimer **3**b-calc. (Fig. 8), the J value diminishes to $+3.9\ \mathrm{cm}^{-1}$, and an inter-dinuclear J_{inter} coupling constant of $-0.10\ \mathrm{cm}^{-1}$ can be found. Since many intermolecular interactions can be established by a single dinuclear unit, it would be expected that these interactions were responsible for the very weak antiferromagnetic behavior of **3**. It should be noted at this point that in the case of molecules formed by fragments with well localized charges (for instance, the BTA anion of **3**) there exist some problems for the theoretical calculation of the energy, and therefore for the evaluation of J. Because of this, the calculated J value could actually be much smaller than $+3.9\ \mathrm{cm}^{-1}$. If so, the set of weak interdinuclear *AF* magnetic interactions transmitted by the hydrogen bonds pathways could overcome the interdinuclear *F* one and an overall *AF* magnetic coupling would be observed in good agreement with the experimental results. This fact is also present in compound $[\mathrm{Cu_2(TzC)_2(H_2O)_6}]$ [21].

The J values can be expressed as the sum of the ferro- and antiferromagnetic contributions, J_{F} and J_{AF}, respectively [24]. When the AF contribution is smaller than the F one, a ferromagnetic coupling can be achieved. Given that the AF contribution can be expressed

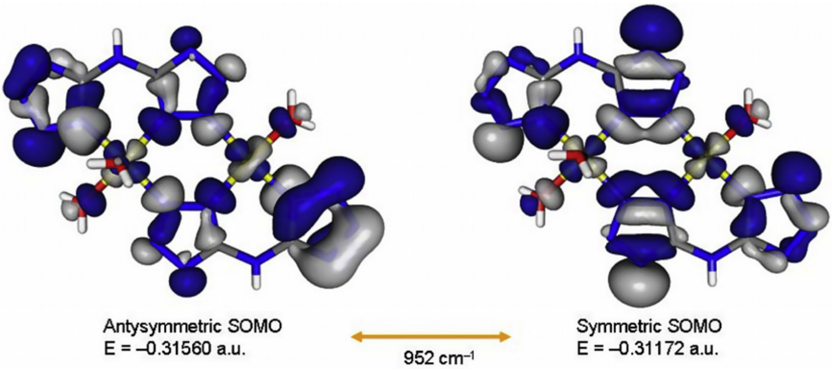

Fig. 9. Symmetric and antisymmetric SOMOs calculated for **3**-calc.

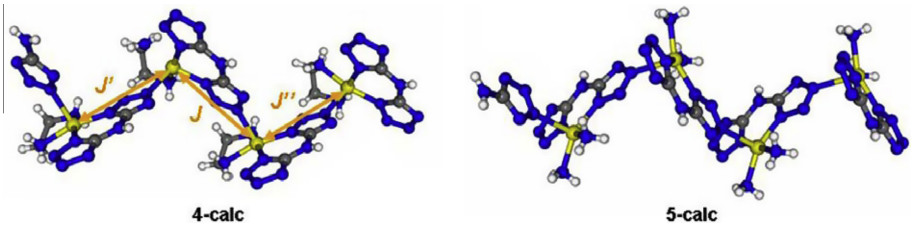

4-calc 5-calc

Fig. 10. The fragments calculated for complexes **4** and **5**, showing the following *J* scheme.

as a function of the square of the SOMOs gap (Δ), the calculated *J* value would point to a low value for the SOMOs splitting. In effect, the energy difference between both single-occupied orbitals in **3**-calc. (Fig. 9) is only 852 cm^{-1} (about 0.1 eV), just on the lower-limit for an antiferromagnetic coupling, following the criterion of Hay et al. for dicopper(II) complexes [24,25] and, therefore, a weak ferromagnetic interaction could appear, supporting our theoretical findings.

The corresponding calculated spin densities for **3**-calc. and **3**b-calc. are depicted in Fig. SI4, showing that the main spin density is, as expected, located at the $dx^2 - y^2$ copper(II) orbitals (+0.6737 e in **3**-calc., and |0.6784| and |0.6709| *e* for each dinuclear unit in **3**b-calc.) accompanied of a significant σ-type spin density delocalisation toward the neighbor nitrogen atoms.

For complex **4**, a quintuplet ground state with a *J* value of +2.0 cm^{-1} has been calculated on considering the fragment **4**-calc. (Fig. 10) formed by four copper(II) centers. This value has been evaluated for the two central copper atoms, which are the more chain-like owing to their inner positions. The two peripheral coupling constants of the model, namely *J′* and *J″* (Fig. 10) are +1.0 and +2.3, respectively. All these values are in perfect agreement with the experimental one (+0.23 cm^{-1}). As indicated above, these results are quite in line with those obtained for the chain $[Cu(BTA)(NH_3)_2]_n$ (**5**), 7 which experimentally showed a weak antiferromagnetic coupling ($J = -7.82\ cm^{-1}$) based on the same considerations of orthogonality of the single occupied copper(II) *d* orbitals.

However, this value seems to be too high from the calculations carried out by us. Thus, taking as model the tetranuclear unit **5**-calc. (Fig. 10), which corresponds with the same fragment as for compound **4**, we have calculated a *J* value of $-0.6\ cm^{-1}$ for the two inner copper centers, and peripheral coupling constants *J′* and *J″* of −0.9 and $-0.2\ cm^{-1}$. Therefore, calculations demonstrate that in both cases the coupling constants are close to zero, since the exchange pathways are poor mediator of the magnetic exchange interaction. The difference in sign between the two BTA-based chains, **4** and **5**, could be due to the different distortion of their respective CuN_5 coordination environments. Thus while **4** exhibits an almost perfect square-pyramid coordination geometry, compound **5** has a geometry that is intermediate between square-pyramidal and trigonal bipyramidal ($\tau = 0.36$). Since for this latter geometry the magnetic orbital is of the dz^2 type, which has 2/3 of its spin density directed to axial positions, there will be some degree of overlapping between the magnetic orbitals on neighboring copper atoms through the tetrazole bridging group. This overlap would lead to a significant antiferromagnetic contribution that would predominate over the ferromagnetic one and, therefore, a overall antiferromagnetic coupling, even though small, would be observed.

The corresponding spin-densities representations for **4** and **5**-calc. are shown in Fig. SI5, which justify the small magnetic coupling by the absence of spin density through the locally perpendicular (*z*) direction following the unique exchange pathways between the copper atoms. Instead, the spin density delocalises in the *xy* plane toward the neighbor nitrogen atoms. The calculated spin densities on the copper centres are +0.6038, +0.6262, +0.6222 and +0.6404 for **4**-calc., and +0.6499, –0.6442, +0.6423 and −0.6328 for **5**-calc. (in both cases, on going from the left to the right in Fig. 10 or Fig. SI5).

4. Conclusions

We present the syntheses and structures of four novel copper(II) complexes containing the bis(5-tetrazolyl)amine ligand (H_2BTA), which show a wide range of structural diversity. Moreover, studies about magnetic properties and DFT calculations of two of these complexes have been performed. Dinuclear and chain coordination complexes exhibit antiferromagnetic and very weak ferromagnetic interactions, respectively. We have used DFT calculations to theoretically determine the sign and value of magnetic couplings exhibited in these compounds. The magnetic exchange couplings for **4** and the analogous complex $[Cu(BTA)(NH_3)_2]_n$ (that exhibits a similar structure and weak AF interaction between the copper(II) ions) have been compared and the differences in magnetic behavior between these compounds have been ascribed to different degree of distortion of their respective CuN_5 coordination environments.

Acknowledgments

This work was supported by the MEC (Spain; Project CTQ-2008-02269/BQU), the Junta de Andalucía (FQM-4228). We would like to thank the Centro de Supercomputación de la Universidad de Granada (UGRGRID) for computational resources.

Appendix A. Supplementary data

Supplementary material CCDC 790132–790135 contains the supplementary crystallographic data for the complexes **1**–**4**. These data can be obtained free of charge from The Cambridge Crystallographic Data Centre via www.ccdc.cam.ac.uk/data_request/cif. Supplementary data associated with this article can be found, in the online version, at doi:10.1016/j.ica.2011.12.040.

References

[1] C. Jiang, Z.P. Yu, S. Wang, C. Jiao, J.M. Li, Z.Y. Wang, Y. Cui, Eur. J. Inorg. Chem. (2004) 3662;
(a) R.G. Xiong, X. Xue, H. Zhao, X.Z. You, B.F. Abrahams, Z. Xue, Angew. Chem., Int. Ed. 41 (2002) 3800;
(b) C. Jiang, X.-J. Mo, E.-Q. Gao, Z. He, W.J. Li, C.H. Yan, Inorg. Chem. Commun. 7 (2004) 353;
(c) T. Wu, B.-H. Yi, D. Li, Inorg. Chem. 44 (2005) 4130;
(d) T.-T. Luo, H.-L. Tsai, S.L. Yang, Y.H. Liu, R.D. Yadav, C.-C. Su, C.-H. Ueng, L.-G. Lin, K.-L. Lu, Angew. Chem., Int. Ed. 44 (2005) 6063;
(e) P. Lin, W. Clegg, R.W. Harrington, R.A. Henderson, Dalton Trans. (2005) 2388;
(f) T. Wu, R. Zhou, D. Li, Inorg. Chem. Commum. 9 (2006) 341;
(g) X. He, C.-Z. Lu, D.-Q. Yuan, Inorg. Chem. 45 (2006) 5760;
(h) A. Rodríguez-Diéguez, E. Colacio, Chem. Commun. (2006) 4140.;
(i) M. Dinca, A.F. Yu, J.R. Long, J. Am. Chem. Soc. 128 (2006) 8904;

(j) M. Dinca, J.R. Long, J. Am. Chem. Soc. 129 (2007) 11172;
(k) M. Dinca, W.S. Han, Y. Liu, A. Dailly, C.M. Brown, J.R. Long, Angew. Chem., Int. Ed. 46 (2007) 1419;
(l) T.M. Klapötke, C.M. Sabaté, M. Rasp, Dalton Trans. (2009) 1825;
(m) P. Pachfule, Y. Chen, C. Sahoo, C. Subash, J. Jiang, R. Banerjee, Chem. Mater. 23 (2011) 2908;
(n) W. Ouellette, S. Jones, J. Zubieta, CrystEngComm 13 (2011) 4457;
(o) E. Yang, Y. Feng, Z. Liu, T. Liu, X. Zhao, CrystEngComm 13 (2011) 230.
[2] (a) Z.P. Demko, K.B. Sharpless, J. Org. Chem. 66 (2001) 7945;
(b) Z.P. Demko, K.B. Sharpless, Org. Lett. 3 (2001) 4091;
(c) F. Himo, Z.P. Demko, L. Noodleman, J. Am. Chem. Soc. 124 (2002) 12210.
[3] (a) A.F. Stassen, H. Kooijman, A.L. Spek, L.J. de Jongh, J.G. Haasnoot, J. Reedijk, Inorg. Chem. 41 (2002) 6468;
(b) C.M. Grunert, P. Weinberger, J. Schweifer, C. Hampel, A.F. Stassena, K. Mereiter, W. Linert, J. Mol. Struct. 733 (2005) 41;
(c) A.S. Lyakhov, V.E. Matulis, P.N. Gaponik, S.V. Voitekhovich, O.A. Ivashkevich, J. Mol. Struct. 876 (2008) 260;
(d) M.X. Peng, C.J. Li, M.L. Tong, Inorg. Chem. Commun. 11 (2008) 707.
[4] A. Rodríguez, R. Kivekäs, E. Colacio, Chem. Commun. (2005) 5228;
(a) J.-R. Li, Q. Yu, C.E. Sañudo, Y. Tao, W.-C. Song, X.-H. Bu, Chem. Mater. 20 (2008) 1218;
(b) A. Rodríguez-Diéguez, M.A. Palacios, A. Sironi, E. Colacio, Dalton Trans. (2008) 2887.
[5] J.Y. Zhang, A.-L. Cheng, Q. Yue, W.-W. Sun, E.-Q. Gao, Chem. Commun. (2008) 847.
[6] A. Rodríguez-Diéguez, A. Salinas-Castillo, S. Galli, N. Masciocchi, J.M. Gutiérrez-Zorrilla, P. Vitoria, E. Colacio, Dalton Trans. (2007) 1821.
[7] (a) M. Friedrich, J.C. Gálvez-Ruiz, T.M. Klapötke, P. Mayer, B. Weber, J.J. Weigand, Inorg. Chem. 44 (2005) 8044;
J.-M. Lin, B.-S. Huang, Y.-F. Guan, Z.-Q. Liu, D.-Y. Wang, Wen. Dong, Cryst. Eng. Comm 11 (2009) 329;
(b) Y.-F. Guan, A.-J. Zhou, D.-Y. Wang, J. Wang, W. Dong, J. Mol. Struct. 938 (2009) 150.
[8] (a) J.-M. Lin, Y.-F. Guan, D.-Y. Wang, W. Dong, X.-T. Wang, S. Gao, Dalton Trans. (2008) 6165;
(b) Y.-B. Lu, M.-S. Wang, W.-W. Zhou, G. Xu, G.-C. Guo, J.-S. Huang, Inorg. Chem. 47 (2008) 8935;
(c) N. Liu, Q. Yue, Y.-Q. Wang, A.-L. Cheng, E.-Q. Gao, Dalton Trans. (2008) 4621.
[9] V.Y. Zubarev, R.E. Trifonov, V.V. Poborchii, Chem. Heterocyclic Comp. 42 (2006) 469.
[10] Bruker Apex2, Bruker AXS Inc., Madison, Wisconsin, USA (2004).
[11] G.M. Sheldrick, SADABS, Program for Empirical Adsorption Correction, Institute for Inorganic Chemistry, University of Göttingen, Germany (1996).
[12] A. Altomare, M.C. Burla, M. Camilla, G.L. Cascarano, C. Giacovazzo, A. Guagliardi, A.G.G. Moliterni, G. Polidori, R. Spagna, J. Appl. Crystallogr. 32 (1999) 115.
[13] G.M. Sheldrick, SHELX97, Program for Crystal Structure Refinement, University of Göttingen, Göttingen, Germany, 1997.
[14] (a) A.D. Becke, Phys. Rev. A 38 (1988) 3098;
(b) C.T. Lee, W.T. Yang, R.G. Parr, Phys. Rev. B 37 (1988) 785;
(c) A.D. Becke, J. Chem. Phys. 98 (1993) 5648.
[15] M.J. Frisch, G.W. Trucks, H.B. Schlegel, G.E. Scuseria, M.A. Robb, J.R. Cheeseman, J.J.A. Montgomery, T. Vreven, K. Kudin, J.C. Burant, J.M. Millam, S.S. Iyengar, J. Tomasi, V. Barone, B. Mennucci, M. Cossi, G. Scalmani, N. Rega, G.A. Petersson, H. Nakatsuji, M. Hada, M. Ehara, K. Toyota, R. Fukuda, J. Hasegawa, M. Ishida, T. Nakajima, Y. Honda, O. Kitao, H. Nakai, M. Klene, X. Li, J.E. Knox, H.P. Hratchian, J.B. Cross, V. Bakken, C. Adamo, J. Jaramillo, R. Gomperts, R.E. Stratmann, O. Yazyev, A.J. Austin, R. Cammi, C. Pomelli, J.W. Ochterski, P. Ayala, K. Morokuma, G.A. Voth, P. Salvador, J.J. Dannenberg, V.G. Zakrzewski, S. Dapprich, A.D. Daniels, M.C. Strain, O. Farkas, D.K. Malick, A.D. Rabuck, K. Raghavachari, J.B. Foresman, J.V. Ortiz, Q. Cui, A. Baboul, S. Clifford, J. Cioslowski, B.B. Stefanov, G. Liu, A. Liashenko, P. Piskorz, I. Komaromi, L. Martin, D.J. Fox, T. Keith, M.A. Al-Laham, C.Y. Peng, A. Nanayakkara, M. Challacombe, P.M.W. Gill, B. Johnson, W. Chen, M.W. Wong, C. Gonzalez, J.A. Pople, In GAUSSIAN 03, Revision C.02, GAUSSIAN, Inc., Wallingford CT (2004).
[16] G.B. Bacskay, Chem. Phys. 61 (1981) 385.
[17] A. Schäfer, C. Huber, R.J. Ahlrichs, Chem. Phys. 100 (1994) 5829.
[18] Jaguar 7.6, Schrödinger, Inc., Portland OR (2009).
[19] (a) E. Ruiz, J. Cano, S. Alvarez, P. Alemany, J. Comput. Chem. 20 (1999) 1391;
(b) E. Ruiz, S. Alvarez, A. Rodríguez-Fortea, P. Alemany, Y. Puoillon, C. Massobrio, in: J.S. Miller, M. Drillon (Eds.), Magnetism: Molecules to Materials, vol. 2, Wiley-VCH, Weinheim, 2001, p. 5572;
(c) E. Ruiz, A. Rodriguez-Fortea, J. Cano, S. Alvarez, P. Alemany, J. Comput. Chem. 24 (2003) 982;
(d) E. Ruiz, S. Alvarez, J. Cano, V. Polo, J. Chem. Phys. 123 (2005) 164110.
[20] A.W. Addison, T.N. Rao, J. Reedijk, J.J. van Rijn, Chem. Soc. Dalton Trans. (1984) 1349.
[21] A. Rodríguez-Diéguez, A.J. Mota, J. Cano, J. Ruiz, D. Choquesillo-Lazarte, E. Colacio, Dalton Trans. (2009) 6335.
[22] (a) A.S. Lyakhov, P.N. Gaponik, M.M. Degtyarik, L.S. Ivashkevich, Acta Crystallogr. C59 (2003) m204;
(b) A.M. Mills, K. Flinzner, A.F. Stassen, J.G. Haasnoot, A.L. Spek, Acta Crystallogr. C58 (2002) m243;
(c) L.S. Ivashkevich, A.S. Lyakhov, P.N. Gaponik, A.N. Bogatikov, A.A. Govorova, Acta Crystallogr. E57 (2001) m335;
(d) G. Gökaugac, L. Tatar, D. Kisakürek, D. Ulkü, Acta Crystallogr. C55 (1999) 1413;
(e) L. Tatar, G. Gökagac, D. Ulkü, Acta Crystallogr. E56 (2000) m335.
[23] G.A. Baker, G.S. Rushbrooke, H.E. Gilbert, Phys. Rev. A 135 (1964) 1272.
[24] P.J. Hay, J.C. Thibeault, R. Hoffman, J. Am. Chem. Soc. 97 (1975) 4884.
[25] D.-B. Kang, Bull. Korean Chem. Soc. 31 (2010) 1704.